Supplement of Hydrol. Earth Syst. Sci., 30, 1463–1485, 2026
https://doi.org/10.5194/hess-30-1463-2026-supplement

Hydrology and Earth System Sciences
Open Access
EGU

Supplement of

Future changes in seasonal drought in Australia

Anna M. Ukkola et al.

Correspondence to: Anna M. Ukkola (a.ukkola@unsw.edu.au)

Figure S1: Location of 216 CAMELS-AUS catchments (in green) used to evaluate AWRA-L historical hydrological drought simulations.

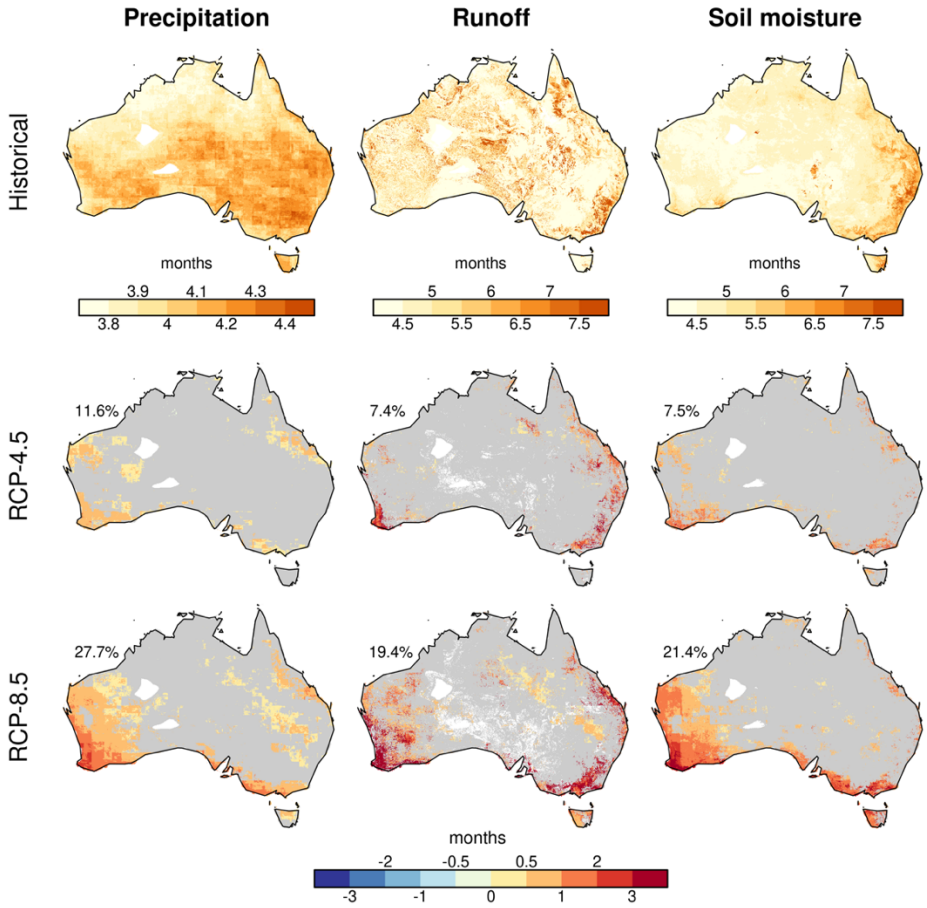

Figure S2: (top) Historical average drought duration for 1970-2005, for precipitation, runoff and soil moisture. (middle, bottom) Change in average drought duration from the 1970-2005 period to the 2064-2099 period under the RCP4.5 and RCP8.5 emission scenarios respectively. Pixels where models do not agree on the change are shown in grey. The percentage shown on the top left of each map represents the percentage of the land area for which models agree on the change. Pixels where drought metrics could not be determined due to a large number of zero values are masked in white.

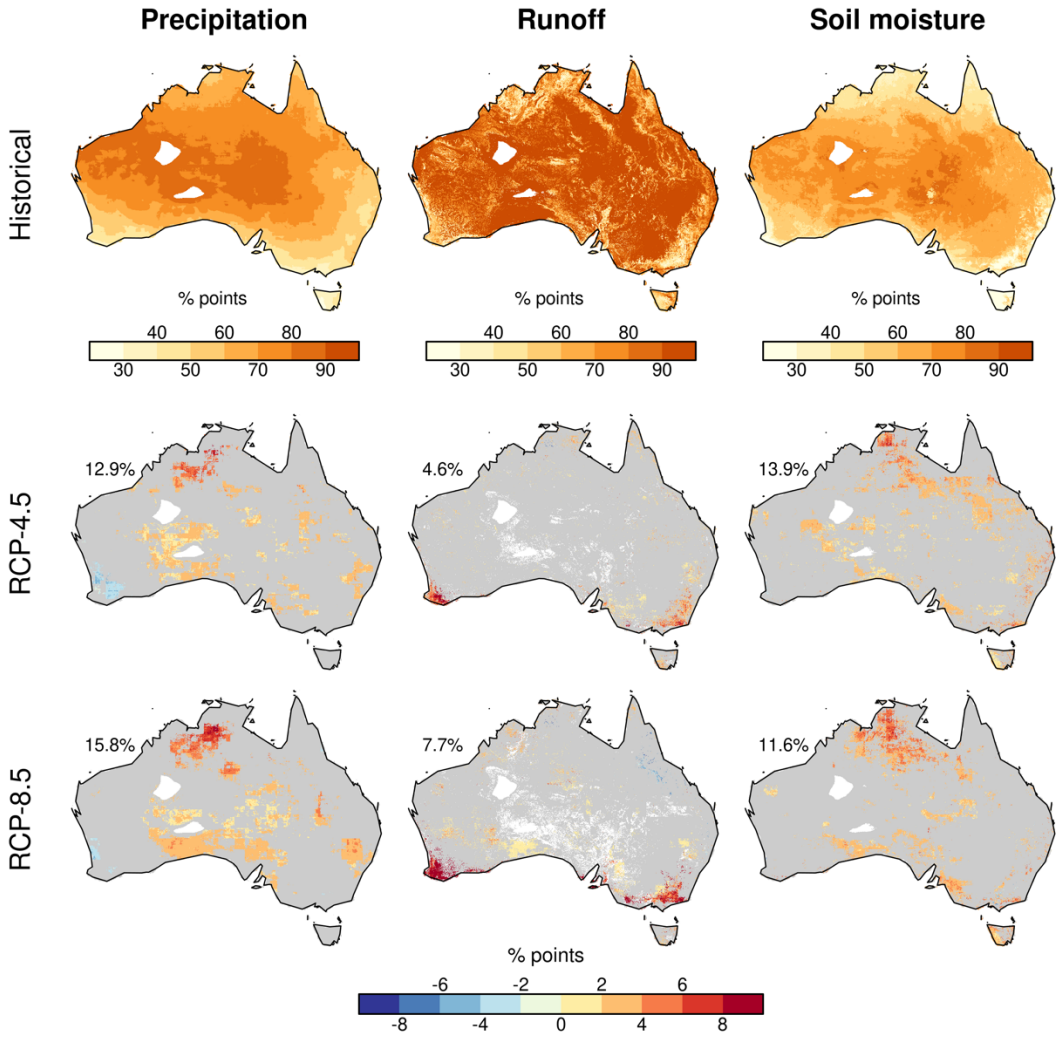

Figure S3: (top) Historical average drought intensity for 1970-2005, for precipitation, runoff and soil moisture. (middle, bottom) Change in average drought duration from the 1970-2005 period to the 2064-2099 period under the RCP4.5 and RCP8.5 emission scenarios respectively. Pixels where models do not agree on the change are shown in grey. The percentage shown on the top left of each map represents the percentage of the land area for which models agree on the change. Pixels where drought metrics could not be determined due to a large number of zero values are masked in white.

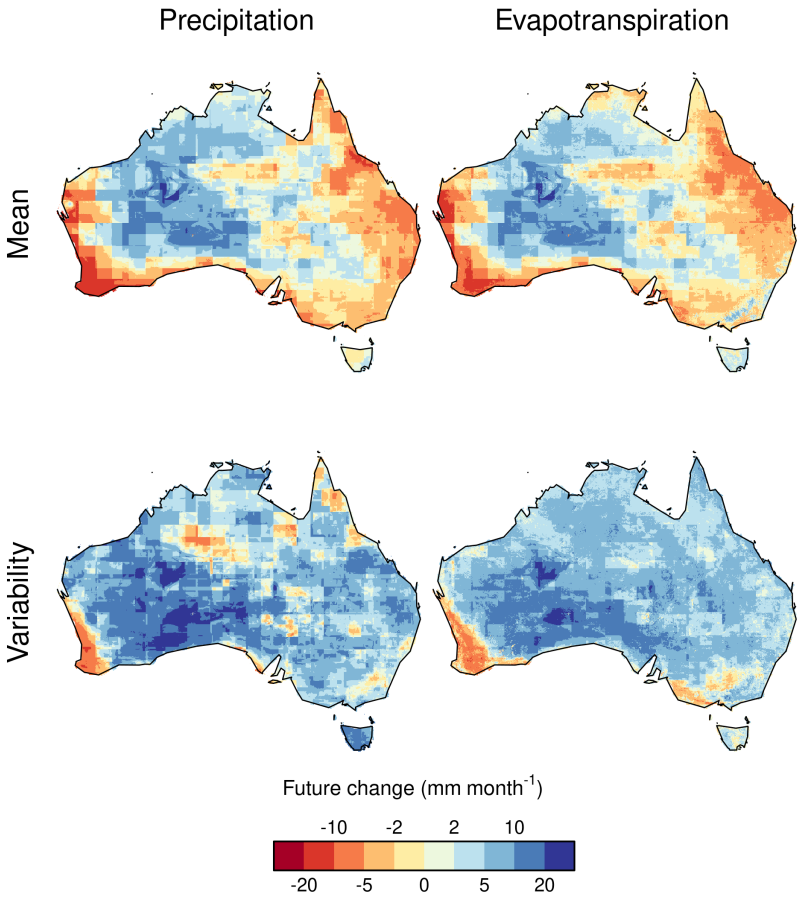

Figure S4: Future changes in mean (top row) and variability (bottom row) of 3-month running mean precipitation and actual evapotranspiration under the RCP4.5 scenario. Variability was quantified from the change in standard deviation of precipitation and ET. The future change was calculated as the difference between the mean and standard deviation during 2064-2099 and 1970-2005.

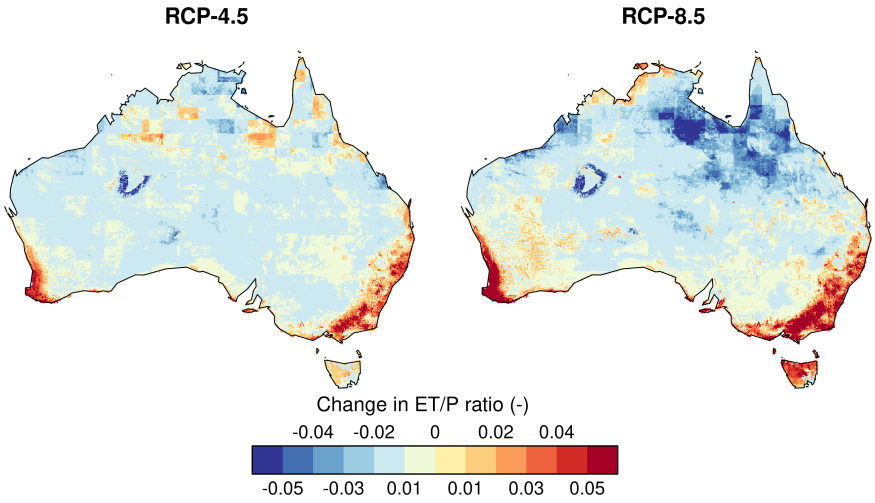

Figure S5: Future change in the mean ratio between actual evapotranspiration (ET) and precipitation (P) under the RCP4.5 and RCP8.5 scenarios. The future change was calculated as the difference between 2064-2099 and 1970-2005 mean ET/P ratios.

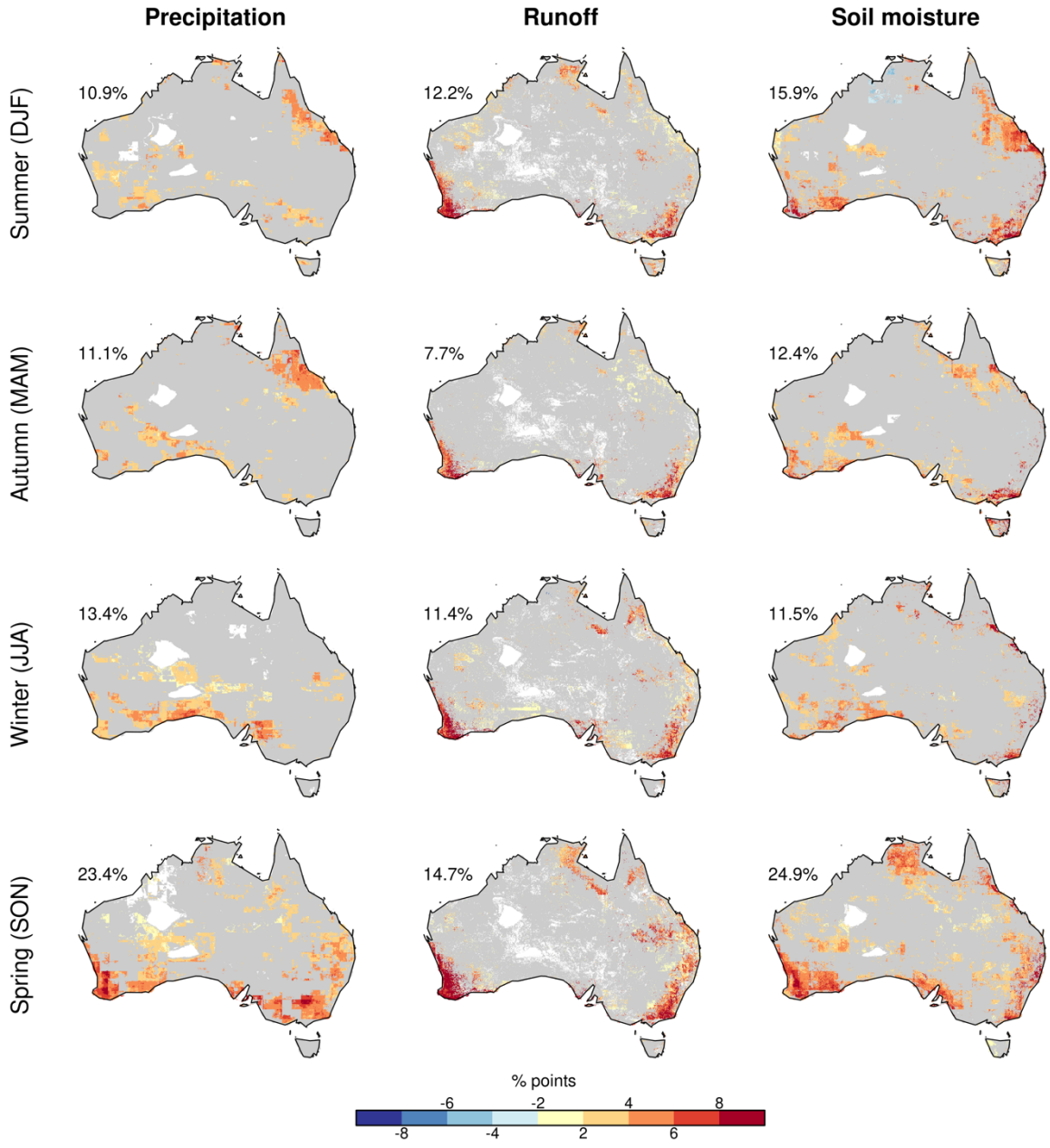

Figure S6: The ensemble mean future change in drought intensity by season for the three drought types under the RCP4.5 scenario. The maps show the difference in time under drought in 2064-2099 compared to the 1970-2005 baseline during each season. Pixels where models do not agree on the change are shown in grey. The percentage shown on the top left of each map represents the percentage of the land area for which models agree on the change. Pixels where drought metrics could not be determined due to a large number of zero values are masked in white.

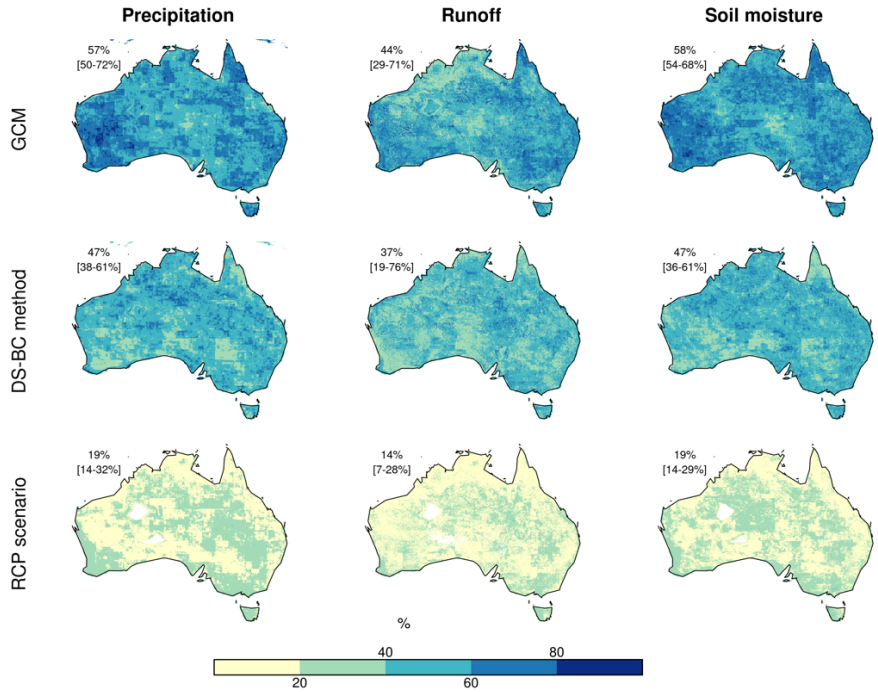

Figure S7: Fraction of total uncertainty arising from the choice of GCM (top row), DS-BC method (middle) and RCP scenario (bottom) for drought duration. The RCP4.5 scenario was used to partition GCM and DS-BC uncertainty (see Methods). The percentage shown on the top left of each map represents the mean fraction of uncertainty averaged across all pixels. The numbers in square brackets show the range in the mean value from the different model combinations (see Methods).

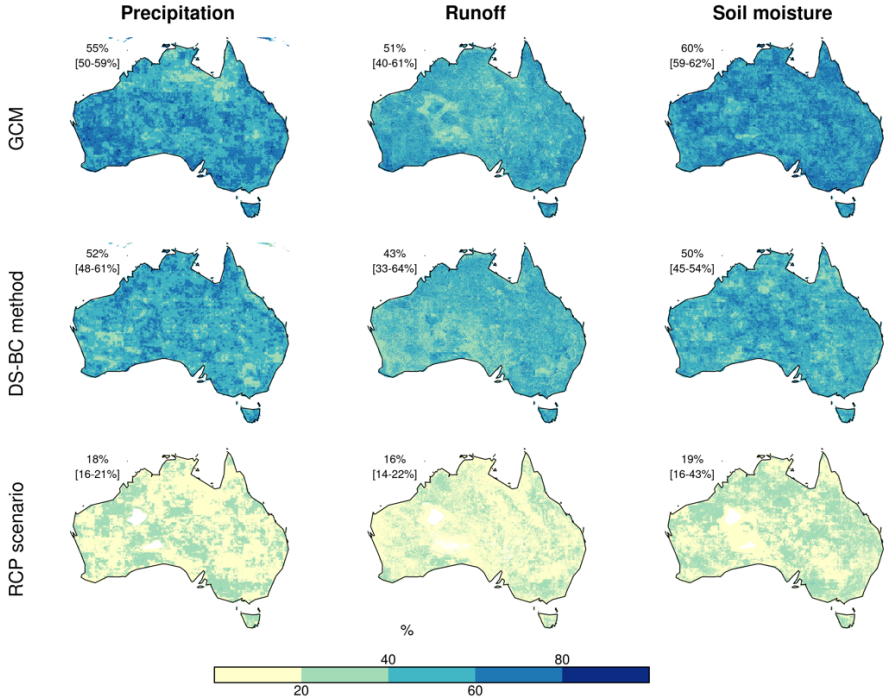

Figure S8: Fraction of total uncertainty arising from the choice of GCM (top row), DS-BC method (middle) and RCP scenario (bottom) for drought intensity. The RCP4.5 scenario was used to partition GCM and DS-BC uncertainty (see Methods). The percentage shown on the top left of each map represents the mean fraction of uncertainty averaged across all pixels. The numbers in square brackets show the range in the mean value from the different model combinations (see Methods).

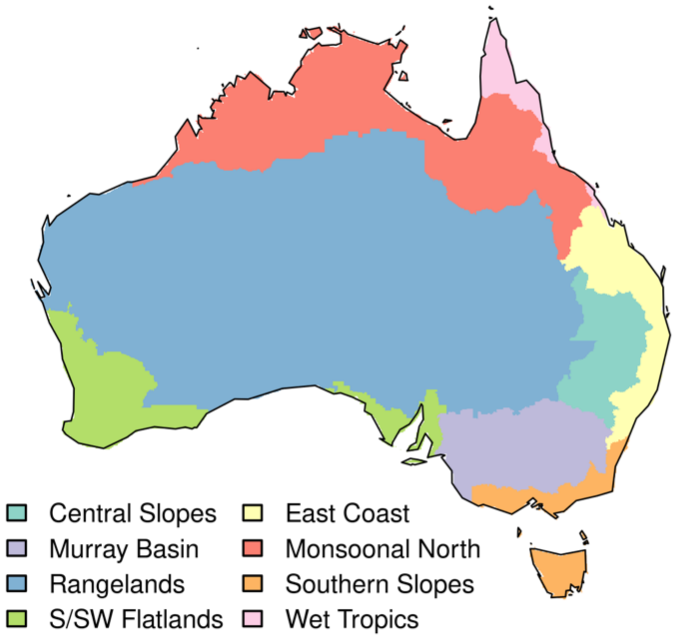

Figure S9: Natural Resource Management (NRM) regions.

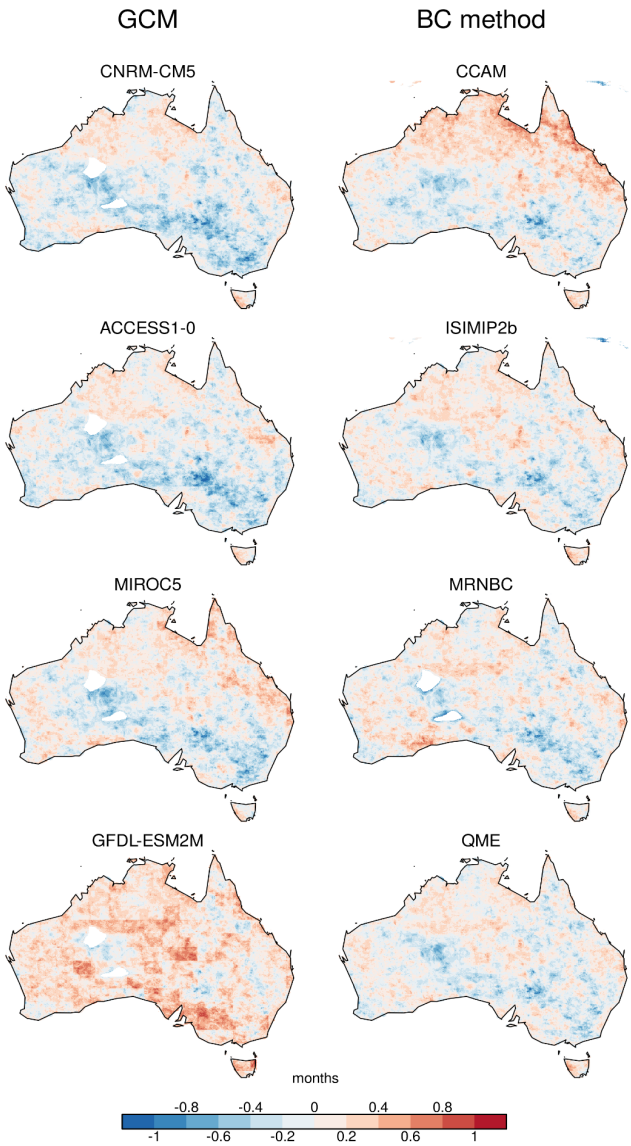

Figure S10: Historical biases in average precipitation drought duration compared to AGCD observations. Data for 1970-2020 was used, with model simulations extended using RCP4.5. Left column shows the average bias in the ensemble members using the same GCM and right column the ensemble members using the same DS-BC method.

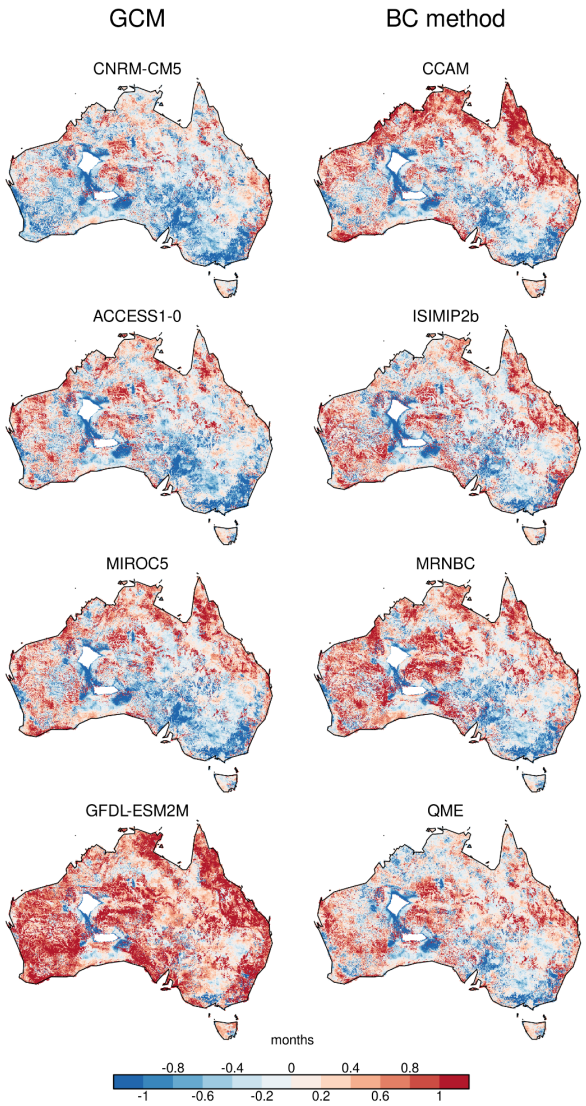

Figure S11: Historical biases in average runoff drought duration compared to the AWRA-L reference simulation. Data for 1970-2020 was used, with NHP model simulations extended using RCP4.5. Left column shows the average bias in the ensemble members using the same GCM and right column the ensemble members using the same DS-BC method.

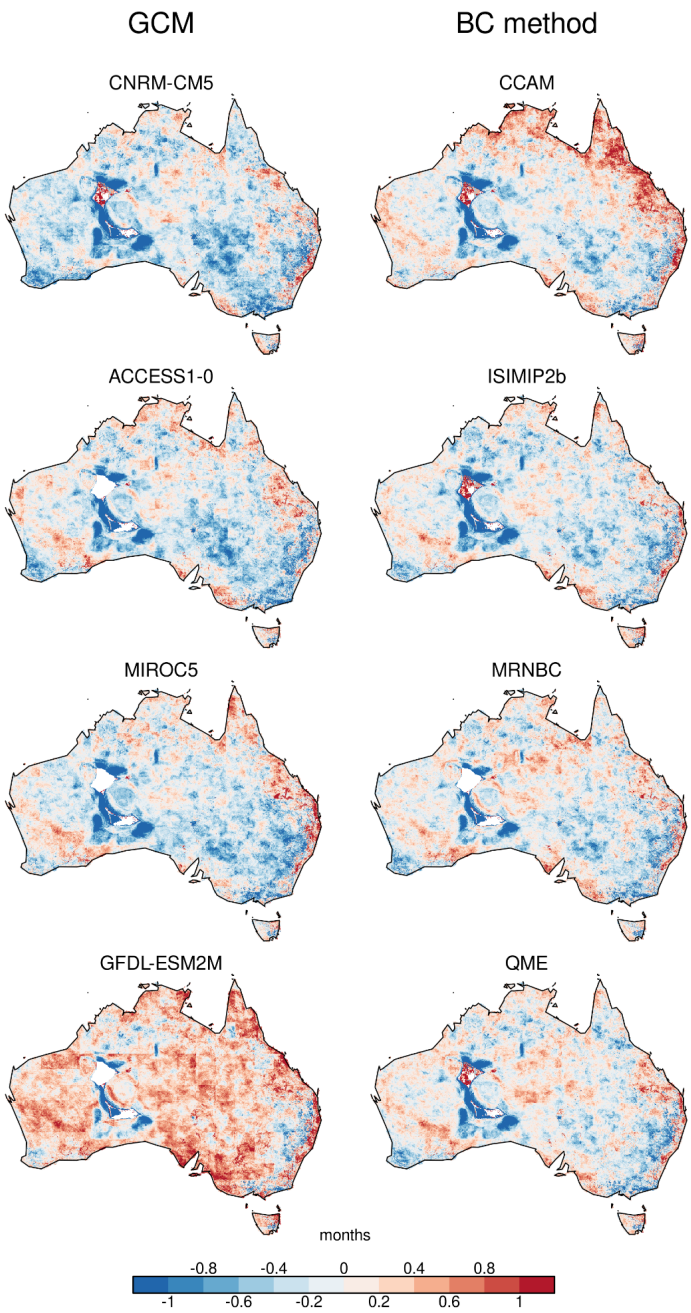

Figure S12: Historical biases in average soil moisture drought duration compared to the AWRA-L reference simulation. Data for 1970-2020 was used, with NHP model simulations extended using RCP4.5. Left column shows the average bias in the ensemble members using the same GCM and right column the ensemble members using the same DS-BC method.

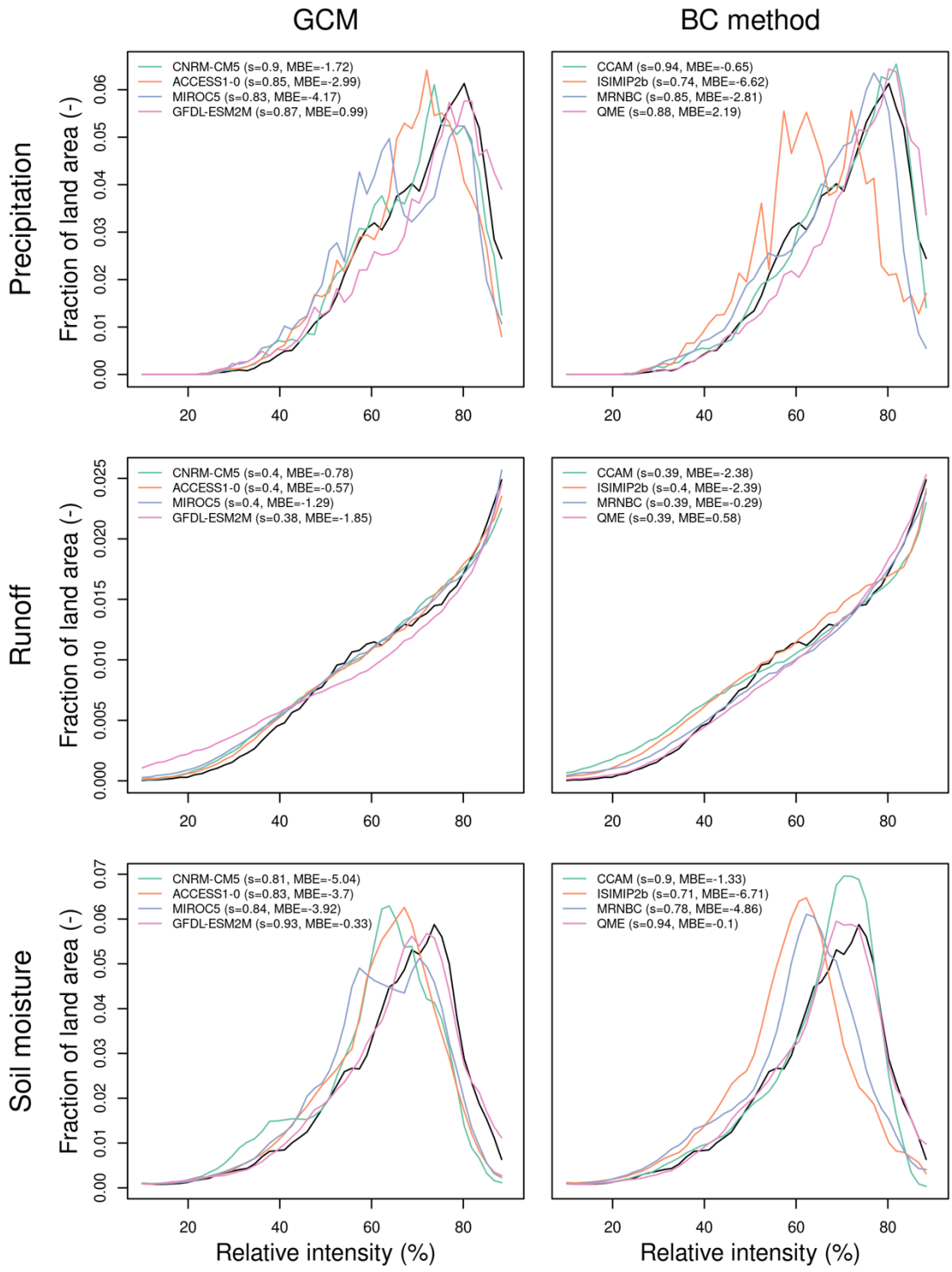

Figure S13: The density distribution of historical drought intensity across all pixels for precipitation, runoff and soil moisture drought (rows). For precipitation, observations are shown in black. For runoff and soil moisture, the observationally-forced historical AWRA-L reference run is shown in black. For each GCM, the data were averaged across the four bias correction members before plotting. For bias correction methods, data were averaged across the four GCMs before plotting. Data for 1970-2020 was used to coincide with the observational data, with the historical model simulations extended using RCP4.5. The Perkins skill score (s) and mean bias error (MBE) are shown for each GCM and bias correction method in the legend.

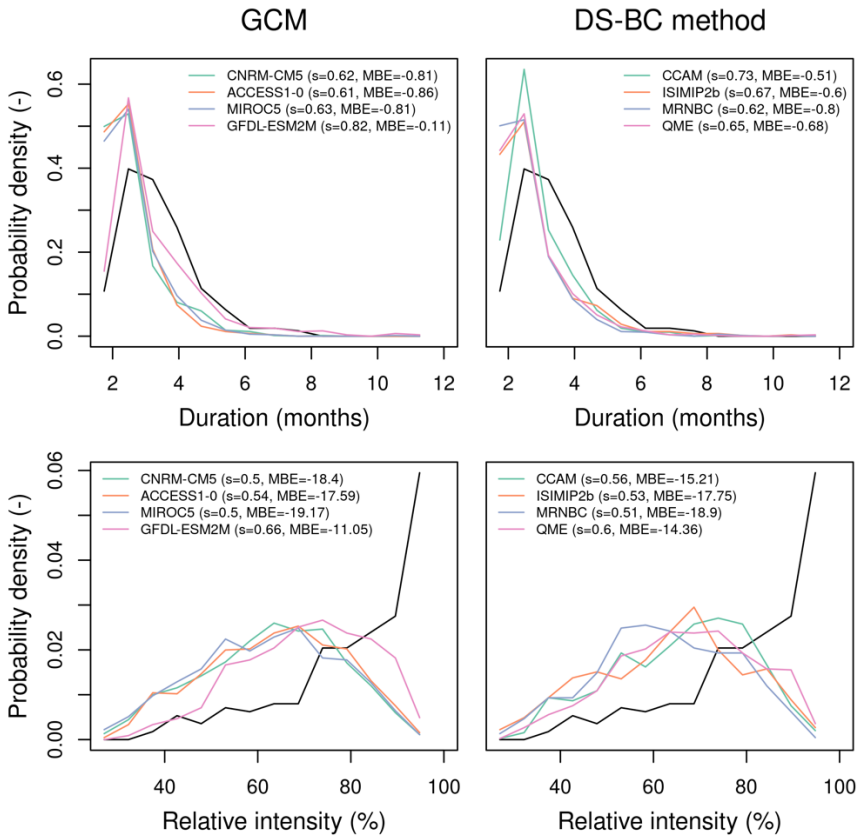

Figure S14: The density distribution of historical drought duration (top row) and intensity (bottom row) across 216 river catchments. Observations from streamflow gauges are shown in black. For each GCM, the data were averaged across the four DS-BC members before plotting. For DS-BC methods, data were averaged across the four GCMs before plotting. Data for 1970-2020 were used to coincide with the observational data, with the historical model simulations extended using RCP4.5. AWRA-L runoff outputs were averaged across the catchments for the comparison using area-weighted averaging. The Perkins skill score (s) and mean bias error (MBE) are shown in the legend.